Chapter 17
Fracture Mechanics at Atomic Scales

Takahiro Shimada and Takayuki Kitamura

Abstract Fracture and strength in atomic components are governed by mechanical instabilities at atomic scales associated with irreversible deformations through bond breaking/switching, such as cleavage, dislocation nucleation, and phase transformations of crystal lattices. It is therefore of central importance to determine the critical conditions where atomic structures becomes mechanically unstable. Here we review the state-of-the-art theory for "fracture mechanics of atomic structures" that provides a rigorous description of mechanical instabilities in arbitrary atomic structures under any external loading/constraint. The theory gives the critical instability condition by positivity of the minimum eigenvalue of the Hessian matrix of the total energy with respect to degrees of freedom of the system (i.e., instability criterion), and it successfully provides atomistic insights into fracture in various atomic/nanoscale structures. The review also covers the recent development of theory extended to advanced systems including large-scale, finite temperature, and "multi-physics" instabilities in (ferro-)electric and magnetic materials as functional fracture.

Keywords Mechanical instabilities · Atomic components · Fracture criterion · Nanoscales · Molecular dynamics

17.1 Introduction

Understanding the nature of fracture, a catastrophic failure of materials, remains a major challenge in a wide range of fields including not only mechanical engineering but also physics, materials science, biology, and geophysics, because fracture is both a physically essential phenomenon and a practically inevitable issue that all

T. Shimada (✉) · T. Kitamura
Department of Mechanical Engineering and Science, Kyoto University,
Nishikyo-ku, Kyoto 615-8540, Japan
e-mail: shimada@me.kyoto-u.ac.jp

T. Kitamura
e-mail: kitamura@kues.kyoto-u.ac.jp

materials in all range of scales intrinsically possess and commonly suffer from (Liebowitz 1968; Zhang et al. 2014; Holland and Marder 1999; Kermode et al. 2008; Pons and Karma 2010; Warner et al. 2007; Buehler and Gao 2006; Song and Curtin 2013; Livne et al. 2010; Nalla et al. 2003; Bažant 2002; Rubin 1995; Dombard 2007). Failure of materials is ultimately governed by bond breaking/switching at the atomic level of crystals. Brittle fracture through cleavage of crystal lattice is the simplest and most typical fracture that is associated with bond breaking. Bond switching often induces the slip of atomic planes resulting in nucleation and multiplication of dislocations and phase transformation of crystal lattices, which are closely related to strength of materials. Such a bond breaking/switching and resulting dramatic change in (global or local) atomic structures can be regarded as "mechanical instabilities" of atomic structures, which often accompany irreversible deformations of materials with a sudden drop of the external load. Such mechanical instabilities can be critical in nanoscale/atomic components such as nanofilms, nanotubes, nanowires and nanodots that have recently been developed due to remarkable advancement in manufacturing technology. In such atomic components only a single bond-breaking/switching often leads to immediate fracture or the fatal malfunction due to their ultimately small dimensions. Therefore, it is of central importance to investigate the nature of mechanical instabilities for thorough understanding of characteristic strength and fracture of atomic components.

Born and Huang (1954) and Milstein (1971); Hill and Milstein (1997); Milstein (1980) demonstrated that stability of a perfect crystal can be evaluated on the basis of the elastic constants. These criteria were extended by Wang et al. (1993, 1997, 1995) for finite deformations, where the crystal stability can be expressed as functions of the elastic stiffness coefficients (i.e., B-criterion). Wang's theorem can be successfully applied to, for example, bifurcation from the fcc to bcc structure in metals under tension (Luo et al. 2002; Černý et al. 2004). However, this criterion is primarily effective only for perfect crystals subject to uniform deformation. As an early attempt toward mechanical instability in inhomogeneous structures, Kitamura et al. (1997, 1998); Yashiro and Tomita (2010) have shown that the dislocation nucleation in a Ni nano-wire under tension by applying the criterion to the local crystal lattice. On the other hand, Li et al. (2003, 2002); van Vliet et al. (2003) employed the concept of phonon soft modes to a local site (Λ-criterion). Dmitriev et al. (2005a, b) applied the concept to the low-dimensional components. Thanks to numerous efforts, the mechanical instabilities in atomic structures have been understood to a certain extent. However, these criteria do not maintain rigorousness, because only the energy balance in a local region (i.e., limited degrees of freedom) is taken into account. For the precise evaluation of mechanical instability in an arbitrary atomic system, it is necessary to consider all the degrees of freedom of the entire system.

A theory that considers the energy balance with respect to all the degrees of freedom of atoms has been proposed by Kitamura et al. (2004a, b). This theory rigorously evaluates the criterion of mechanical instability in heterogeneous atomic systems under non-uniform loading or constraint (Kitamura et al. 2004a, b). Here we review the rigorous criterion that describes the mechanical instabilities in arbitrary atomic structures and its recent advances and applications. In Sect. 17.2, we

provide a detailed theory to describe the mechanical instabilities in atomic structures and its applications. In Sect. 17.3, we discuss problems of this original theory for practical situations and introduce an improved approach that resolves the problems. Section 17.4 contributes to the review of recent advances and extension of the method toward complicated system such as finite temperature, electric, and magnetic systems. In Sect. 17.5 we summarize the present review with some future directions of mechanical instability issues.

17.2 Fracture Criterion for Mechanical Instability in Arbitrary Atomic Structures

To investigate the onset and nature of mechanical instabilities in atomic components, a rigorous and universal criterion has been proposed for an arbitrary atomic structure under any loading/constraint condition (Kitamura et al. 2004a, b). Here, let us consider an atomic system consisting of N atoms. The potential energy of the atomic system, Φ, can be represented as a function of atomic coordinate,

$$\Phi = \Phi(\boldsymbol{R}), \tag{17.1}$$

where $\boldsymbol{R}$ denotes the configuration vector consisting of atomic positions,

$$\begin{aligned}\boldsymbol{R} \equiv{}^t &(r_z^2, r_y^3, r_z^3, r_x^4, r_y^4, r_z^4, \ldots, r_i^\alpha, \ldots, r_x^N, r_y^N, r_z^N)\\ ={}^t &(R_1, R_2, \ldots, R_m, \ldots, R_M)\end{aligned} \tag{17.2}$$

Here, r_i^α denotes the coordinate of atom α in the $i (= x, y, z)$ direction. This is the general form to express the potential energy of atomic system, in any type of po-tential functions and force fields including first-principles (quantum-mechanics) approaches. The irreducible number of structural degrees of freedom (DOFs) in the atomic system without any constraint is $M = 3N - 6$ because the DOFs of rigid-body translations (3) and rotations (3) is subtracted from the total DOFs of atoms ($3N$). Under a displacement constraint where some of atoms are fixed, the number of DOFs is $M = 3N - 3n_c - 6$, where n_c is the number of constrained atoms. Here, let us consider the atomic system under static external load, i.e., the atoms are located at their own optimal sites and are in balance with the external load and/or constraint. The total energy Π at the equilibrated atomic configuration ($\boldsymbol{R}_0$) under external load consists of the potential energy, Φ, and the work done by external load, W,

$$\Pi = \Phi + W \tag{17.3}$$

Assuming an infinitesimal deformation, $\delta\boldsymbol{R}$, to the equilibrated system, the total energy of slightly deformed system, $\Pi(\boldsymbol{R}_0 + \delta\boldsymbol{R})$, can be described by the Taylor's series expansion of total energy $\Pi(\boldsymbol{R}_0)$ with respect to $\delta\boldsymbol{R}$,

$$\Pi(\boldsymbol{R}_0 + \delta\boldsymbol{R}) = \Pi(\boldsymbol{R}_0) + \sum_{m=1}^{M} \left(\left.\frac{\partial \Phi}{\partial R_m}\right|_{\boldsymbol{R}=\boldsymbol{R}_0} + \left.\frac{\partial W}{\partial R_m}\right|_{\boldsymbol{R}=\boldsymbol{R}_0} \right) \delta R_m$$

$$+ \frac{1}{2} \sum_{m=1}^{M} \sum_{n=1}^{M} \left.\frac{\partial^2 \Phi}{\partial R_m \partial R_n}\right|_{\boldsymbol{R}=\boldsymbol{R}_0} \delta R_m \delta R_n + \cdots \qquad (17.4)$$

$$+ \frac{1}{2} \sum_{m=1}^{M} \sum_{n=1}^{M} \left.\frac{\partial^2 W}{\partial R_m \partial R_n}\right|_{\boldsymbol{R}=\boldsymbol{R}_0} \delta R_m \delta R_n + \cdots ,$$

where R_m denotes a component of configuration vector $\boldsymbol{R}$ included in the DOFs of system, i.e., $R_m = r_i^\alpha$. Since the first derivative of total energy (i.e., force acting on atoms) is zero due to the system at equilibrium, the second term on the right-hand side can be eliminated

$$\frac{\partial \Pi}{\partial R_m} \delta R_m = \left(\left.\frac{\partial \phi}{\partial R_m}\right|_{\boldsymbol{R}=\boldsymbol{R}_0} + \left.\frac{\partial W}{\partial R_m}\right|_{\boldsymbol{R}=\boldsymbol{R}_0} \right) \delta R_m \qquad (17.5)$$

Considering that the external load is constant due to the static loading, the work is proportional to the displacement of atoms on which the external load is applied. Thus, we obtain

$$\frac{\partial^2 W}{\partial R_m \partial R_n} \delta R_m \delta R_n = 0 \qquad (17.6)$$

Using Eqs. (17.4)–(17.6) and ignoring the higher-order terms, the change in total energy $\delta\Pi$ with respect to the infinitesimal deformation $\delta\boldsymbol{R}$ is given by

$$\delta\Pi(\boldsymbol{R}_0) = \Pi(\boldsymbol{R}_0 + \delta\boldsymbol{R}) - \Pi(\boldsymbol{R}_0) = \frac{1}{2} \sum_{m=1}^{M} \sum_{n=1}^{M} \frac{\partial^2 \Phi}{\partial R_m \partial R_n} \delta R_m \delta R_n = \frac{1}{2} \delta\boldsymbol{R}^T \boldsymbol{H} \delta\boldsymbol{R},$$

$$(17.7)$$

where $\boldsymbol{H}$ is the $M \times M$ Hessian matrix of potential energy Π with respect to $\boldsymbol{R}$, and the superscript ^{T} means transposition. The component of Hessian matrix, H_{mn}, is

$$H_{mn} \equiv \left.\frac{\partial^2 \Phi}{\partial R_m \partial R_n}\right|_{\boldsymbol{R}=\boldsymbol{R}_0} \qquad (17.8)$$

By solving the eigenvalue problem of the Hessian matrix $\boldsymbol{H}$, we obtain

$$\boldsymbol{H}\boldsymbol{p}_m = \eta_m \boldsymbol{p}_m, \qquad (17.9)$$

where η_m is the eigenvalue of the Hessian matrix $\boldsymbol{H}$, and $\boldsymbol{p}_m$ is the corresponding eigenvector. Using the eigenvector $\boldsymbol{p}_m$, the Hessian matrix is diagonalized as

$$P^{-1}HP = P^T HP = \begin{pmatrix} \eta_1 & & 0 \\ & \ddots & \\ 0 & & \eta_M \end{pmatrix}, \qquad (17.10)$$

where $P = (p_1 \ldots p_M)$. Since the eigenvectors are an orthogonal basis set of M-dimensional vector space, any infinitesimal deformation δR can be expressed as a linear combination of the eigenvectors as

$$\delta R = \sum_{m=1}^{M} u_m p_m = Pu, \qquad (17.11)$$

where u_m is the component of δR in the p_m direction, $u = (u_1 \ldots u_M)$. Therefore, the total energy change with δR in Eq. (17.7) becomes

$$\delta \Pi(R_0) = \frac{1}{2}(Pu)^T H(Pu) = \frac{1}{2}u(P^T HP)u = \sum_{m=1}^{M} \eta_m u_m^2 \qquad (17.12)$$

In this equation, the eigenvalue, η_m, signifies the potential energy curvature against the deformation along the corresponding eigenvector, p_m. Therefore, if the minimum eigenvalue is positive ($\eta_1 > 0$), the change in the total energy, $\delta \Pi$, is always positive with respect to any infinitesimal deformation, indicating that the system is mechanically stable. On the other hand, when the minimum eigenvalue becomes zero or negative ($\eta_1 \leq 0$), the total energy can decrease along the corresponding eigenvector, p_1. This indicates that the system is mechanically unstable and the corresponding eigenvector p_1 represents the atomic motion at the beginning of instability (unstable mode). Therefore, the onset of mechanical instabilities in atomic structures can be determined by the positivity of the eigenvalue of Hessian matrix H, i.e., $\eta_1 = 0$ (Kitamura et al. 2004a, b).

The validity of the theory has been verified by applying the criterion to a nanoscale cracked atomic body under external load (Kitamura et al. 2004b), as shown in Fig. 17.1. Two different loading conditions that lead to different fracture modes were applied to the model: the external load-controlled (Case A) and the displacement-controlled (Case B) conditions. Figure 17.2a plots the stress-strain curves of Cases A and B. The two stress-strain curves exhibit the different behavior, especially, the different critical strain where fracture occurs. Note that these bring about different morphology of mechanical instability at the critical strain: the cleavage crack propagation is observed for Case A (i.e., brittle fracture), while the dislocation emission from the crack tip (i.e., ductile fracture) occurs for Case B. The above criterion was applied to these two deformations and fracture, and the minimum eigenvalue as a criterion is evaluated for each case, as shown in Fig. 17.2b. Although the mechanical behavior and fracture mode are totally different between Cases A and B, the minimum eigenvalues become zero at each critical strain where stress dramatically drops (or the strain diverges) and fracture occurs. This indicates that the instability
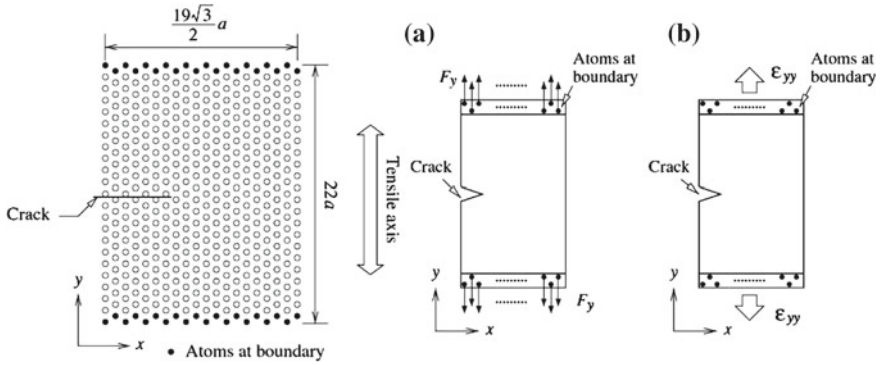
Fig. 17.1 An atomic structure with a crack. **a** Case A: load control simulation. **b** Case B: displacement control simulation (Kitamura et al. 2004b)
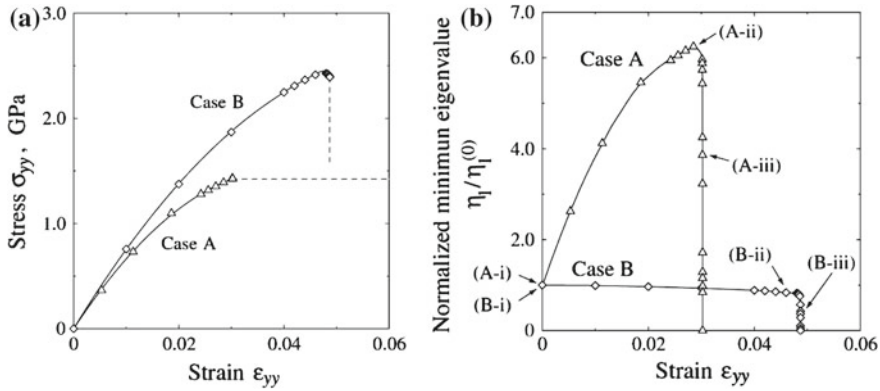

Fig. 17.2 Results of computational tensile tests shown in Fig. 17.1. **a** Stress versus strain curves of cracked atomic structures, **b** minimum eigenvalue normalized by that of unstrained one as a function of strain (Kitamura et al. 2004b)

criterion, $\eta_1 = 0$, exactly captures the critical strain where fracture occurs regardless of the fracture modes.

Figure 17.3 shows the unstable deformation mode, $\boldsymbol{p}_1$, corresponding the minimum eigenvalue of $\eta_1 = 0$. The dominant mode vector for Case A represents the opening mode of crack, i.e., cleavage fracture. On the other hand, the unstable mode of Case B shows the sliding mode of neighboring atomic planes, i.e., the dislocation emission from the crack tip. These modes are perfectly consistent with the fracture behaviors directly obtained by the molecular dynamics simulations. Therefore, the method can rigorously evaluate the instability criterion as well as the deformation mode of the mechanical instabilities.

Owing to the capability of the criterion as a powerful tool to explore the nature of fracture in atomic components, the method has been applied to various kinds of
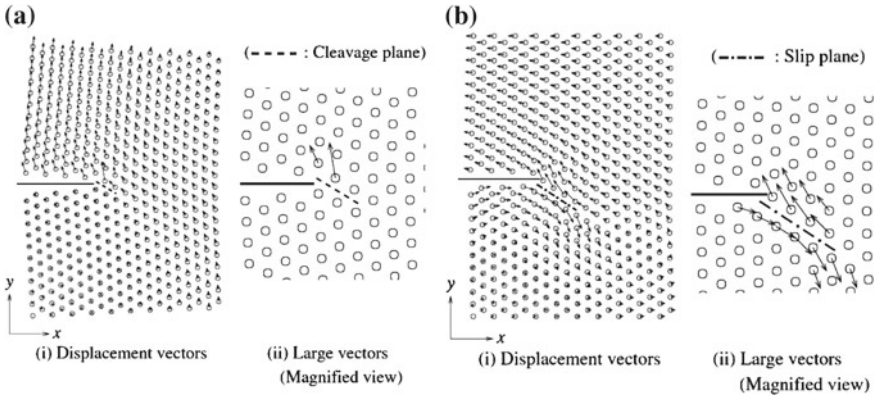
Fig. 17.3 Unstable deformation modes (eigenvectors corresponding to minimum eigenvalues) for **a** Case A and **b** Case B (Kitamura et al. 2004b)

systems (Kitamura et al. 2004a; Umeno et al. 2007; Shimada et al. 2008, 2009a; Kubo et al. 2013), including metallic glasses and amorphous metals (Umeno et al. 2007; Shimada et al. 2008, 2009a), interface cracking of nanofilms (Kitamura et al. 2004a), and sliding and/or switching of domain/grain boundaries (Umeno et al. 2009). For example, the method clarified the fracture mode of bi-material interfaces and its dominant region near the interface edge (Kitamura et al. 2004a), as shown in Fig. 17.4a. The method was also applied to more complicated atomic structures, such as amorphous metals, where atoms are arranged almost randomly in contrast to crystal lattices. Although it was difficult to extract detailed deformation processes that contribute to macroscopic plasticity in amorphous metals due to the random atomic arrangements, the method successfully captured the localized atomic motions dominated by several tens of atoms (see Fig. 17.4b) as an elementary process of plasticity in amorphous metals (Umeno et al. 2007; Shimada et al. 2008, 2009a).
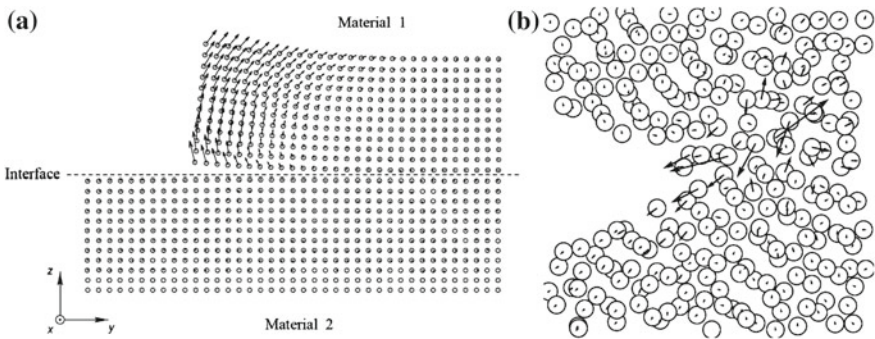
Fig. 17.4 Unstable deformation modes of **a** delamination of bi-material interfaces (Kitamura et al. 2004a) and **b** amorphous metals near a crack-tip (Shimada et al. 2009a)

Thus, the method has successfully revealed the nature of mechanical instabilities at the atomic scales and the elementary process of complicated deformation and fracture in atomic structures.

17.3 Simplified Evaluation of Fracture Criterion for Large-Scale Atomic Structures

Although the applicability of the instability criterion is quite large and a variety of mechanical instabilities and fracture issues can be solved by the theory, there are still some problems. One of the difficulties is to apply the criterion to a large-scale atomic structure. When the system contains huge number of atoms, the DOFs of the system and the resulting Hessian matrix, H, in Eq. (17.8) becomes extremely large so that the eigenvalue problem of Hessian matrix cannot be computationally solved due to its huge memory requirements.

In this section, we introduce a simplified method to evaluate mechanical instabilities even in a large-scale atomic structure using a reasonable concept to re-duce the effective degrees of freedom in the system (Shimada et al. 2009b, 2010b). In an attempt to re-duce the degrees of freedom in the computation, a part of the atomic system is divided into elements and the displacement of atoms in the element is described using a linear function of the nodal coordinate, like the well-established concept of finite element analysis. Figure 17.5 schematizes the concept applied to a three-dimensional atomic structure with a crack (Shimada et al. 2010b). In the area
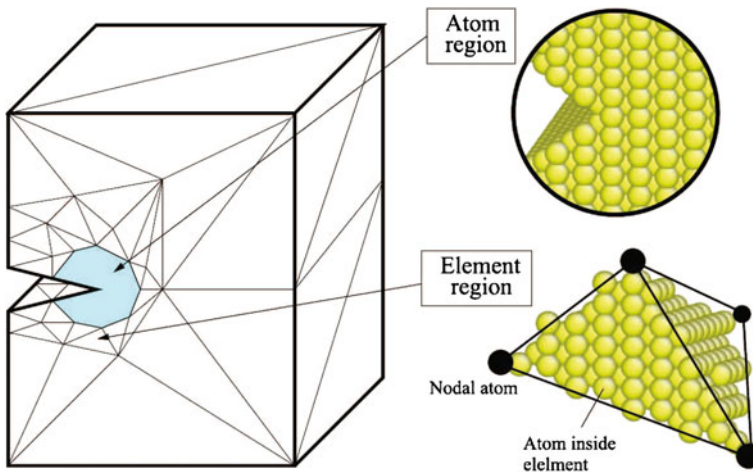
Fig. 17.5 Schematic illustration explaining the concept of reducing degrees of freedom by using linear elements in a three-dimensional atomic structure with a crack. Degrees of freedom of atoms inside an element are represented by its nodal displacement (Shimada et al. 2010b)

far from the crack, the element includes many atoms because the strain gradient is moderate and the deformation of the atoms can be well-described by the nodal displacements of element. On the other hand, the number of atoms in the element should decrease in the region near the crack tip where the strain concentrates, and the DOFs of each atom is fully taken into account in the proximity of the crack-tip where the unstable deformation preferentially occurs.

Denoting the number of atoms and nodes in the system as N'_{atom} and N'_{node}, respectively, we can re-describe the deformation of the system by the vector $\boldsymbol{R}'$,

$$\boldsymbol{R}' \equiv^t \left(r_x^1, r_y^1, r_z^1, \ldots, r_i^\alpha, \ldots, r_x^{N'_{atom}}, r_y^{N'_{atom}}, r_z^{N'_{atom}}, \right.$$
$$\left. S_x^1, S_y^1, S_z^1, \ldots, S_i^\xi, \ldots, S_x^{N'_{node}}, S_y^{N'_{node}}, S_z^{N'_{node}} \right) \tag{17.13}$$

where S_i^ξ denotes the i-th coordinate of a node, ξ. Following the concept of the finite element analyses, it is assumed that the displacements in the x, y, and z direction of an atom α in an element, u_x^α, u_y^α, and u_z^α, respectively, can be represented using the linear function as

$$u_x^\alpha = a_1 + a_2 r_x^\alpha + a_3 r_y^\alpha + a_4 r_z^\alpha,$$
$$u_y^\alpha = a_5 + a_6 r_x^\alpha + a_7 r_y^\alpha + a_8 r_z^\alpha, \tag{17.14}$$
$$u_z^\alpha = a_9 + a_{10} r_x^\alpha + a_{11} r_y^\alpha + a_{12} r_z^\alpha,$$

For the node , ξ, we obtain

$$U_x^\xi = a_1 + a_2 S_x^\xi + a_3 S_y^\xi + a_4 S_z^\xi,$$
$$U_y^\xi = a_5 + a_6 S_x^\xi + a_7 S_y^\xi + a_8 S_z^\xi, \tag{17.15}$$
$$U_z^\xi = a_9 + a_{10} S_x^\xi + a_{11} S_y^\xi + a_{12} S_z^\xi,$$

where $U_i^\xi (i = x, y, z)$ denotes the nodal displacement. Thus, the displacement of atoms in the element can be described by the displacements of 4 nodes that consist of the tetrahedral element as follows

$$\begin{Bmatrix} u_x^\alpha \\ u_y^\alpha \\ u_z^\alpha \end{Bmatrix} = C_\alpha^1 \begin{Bmatrix} U_x^1 \\ U_y^1 \\ U_z^1 \end{Bmatrix} + C_\alpha^2 \begin{Bmatrix} U_x^2 \\ U_y^2 \\ U_z^2 \end{Bmatrix} + C_\alpha^3 \begin{Bmatrix} U_x^3 \\ U_y^3 \\ U_z^3 \end{Bmatrix} + C_\alpha^4 \begin{Bmatrix} U_x^4 \\ U_y^4 \\ U_z^4 \end{Bmatrix}, \tag{17.16}$$

where the coefficient of node ξ, C_α^ξ, is represented as a function of the coordinate of atom and node, r_i^α and S_i^α (Shimada et al. 2010b).

The number of reduced degrees of freedom can now be $M' = 3(N'_{atom} + N'_{node}) - 6$ (or, $M' = 2(N'_{atom} + N'_{node}) - 3$ for a two-dimensional system). It should be noted that the reduced DOFs of M' is quite smaller than the original DOFs of atoms M because large number of atoms are included in the element regions (i.e., $M' \ll M$). The Hessian matrix of this atom-element system, $\boldsymbol{H}'$, to be solved is now rewritten as
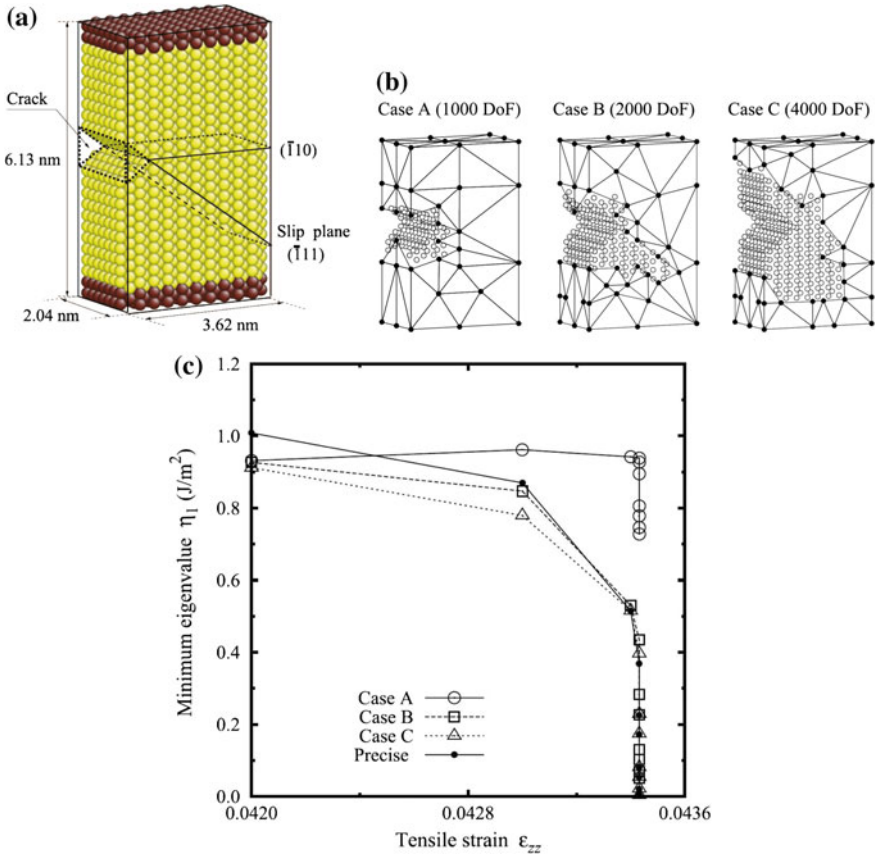
Fig. 17.6 a Three-dimensional atomic structure of Cu with a crack. **b** Elements and atoms for 1000 (Case A), 2000 (Case B), and 4000 (Case C) degrees of freedom generated according to the deformation gradient. Note that the number of degrees of freedom of all atoms is 11127. **b** Minimum eigenvalues normalized by those of the unstrained state as a function of strain obtained by Cases A, B, and C and exact solution of original method as "Precise" (Shimada et al. 2010b)

$$H'_{mn} = \frac{\partial^2 U}{\partial R'_m \partial R'_n}, \qquad (17.17)$$

where the size $(M' \times M')$ is significantly reduced from the original size $(M \times M)$ because $M' \ll M$ (Shimada et al. 2010b). Therefore, by applying the atom-element concept, the eigenvalues (instability criterion) as well as the corresponding eigenvectors (unstable mode) can be computed even in a large-scale atomic structure.

The atom-element concept for the mechanical instability analysis of large-scale atomic structures has been validated by applying the concept to the three-dimensional Cu atomic structure with a crack under tension (Shimada et al. 2010b), as shown in Fig. 17.6a. During tension tests, a dislocation is emitted from the crack tip at a critical

strain. The stress-strain curve and the resulting dislocation emission are similar to those shown in Fig. 17.1 (Case B), although we do not show the details of tensile deformations here. Figure 17.6b shows the mesh division of a three-dimensional atomic component with a crack. The atomic structure is divided into elements according to the strain gradient (Shimada et al. 2009b, 2010b). Here, atomic displacement in an element is linearly related with the displacement at the nodes. The models of Cases A, B, and C have approximately 1000, 2000, and 4000 degrees of freedom, respectively. Note that the total number of degrees of freedom (atomic degrees of freedom) is 11127. The atomic region appears near the crack tip and elements become rough far from the crack. Figure 17.6c plots the minimum eigenvalues of the Hessian matrix for Cases A, B and C. The model with the lowest degrees of freedom (Case A) significantly differs from the exact numerical solution that considers all the degrees of freedom shown as "Precise." On the other hand, by increasing the degrees of freedom, Cases B and C give almost the same curves of the exact solution. Cases B and C are therefore quite good approximation of the exact solution so that we are able to determine the onset of mechanical instability from the minimum eigenvalue with reduced DOFs and Hessian matrix H'.

Figure 17.7 shows the unstable eigenvector modes corresponding to the minimum eigenvalues for Cases A, B, and C. Case A gives a mode that is remarkably deviated from the exact solution. This is because the Case A does not afford enough DOFs to
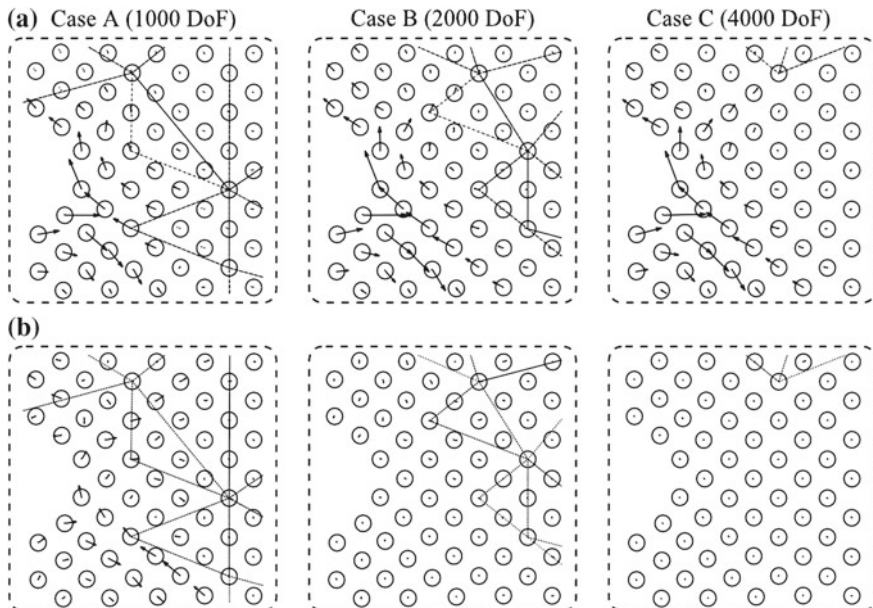
Fig. 17.7 Simplified instability analysis results for Cases A, B, and C. **a** Unstable mode vectors. **b** Error vectors representing the difference from the exact unstable mode. Only the region near the crack tip is shown (Shimada et al. 2010b)

represent the unstable mode of discretized atomic motion near the crack tip. On the other hand, the unstable deformation mode is correctly described when the degrees of freedom is more than 2000 (Case B). Here, the size of matrix, $\boldsymbol{H}'$, is reduced to about 1/25 compared with that of the original approach, $\boldsymbol{H}$. Here, it should be noted that the model introduced here is relatively small for the purpose of the validation of the concept. When we deal with larger atomic structures that contain millions of atoms as molecular dynamics simulations usually treat, a huge number of atoms are included in the element region and the size of Hessian matrix can be reduced dramatically. We also remark that, although the present model has a crystalline structure which is more likely to apply the atom-element concept due to its regular atomic arrangement, it has been confirmed that the concept can be applied to even highly-disordered structures such as amorphous metals where the atomic displacement exhibits quite nonlinear behavior (Shimada et al. 2009a; Kubo et al. 2013). Therefore, the atom-element concept introduced here is quite successful and therefore enables us to evaluate the mechanical instability criterion even for large-scale atomic systems.

17.4 Recent Advances of Instability Criteria for Complicated Systems

Very recently, numerous attempts and efforts have been made to extend and apply the instability criterion to more complicated systems and phenomena (Umeno et al. 2009, 2010; Shimada et al. 2010a; Yan et al. 2012; Shimada et al. 2012, 2015), such as finite temperature, dislocation structures, ferroelectrics, magnetic materials, etc. Especially, it has recently attracted much attention that mechanical stress/strain strongly affects and interacts with ferroelectric and magnetic properties, i.e., "multi-physics" coupling. Nanostructures where the discreteness of atoms becomes dominant exhibit novel multi-physics properties that is distinct from the bulk counterpart, as reviewed in (Shimada and Kitamura 2014). Here, we thus focus on advanced instability criteria related to these hot "multi-physics" phenomena.

For ferroelectric materials where a spontaneous ionic displacement brings about electric dipoles in perovskite lattices, i.e., spontaneous polarization, the spontaneous polarization interacts with external electric field. When the external field exceeds the critical value, the spontaneous polarization and internal ionic displacement becomes unstable and finally switches its directions, namely, do-main switching. Thus, the domain switching is one of instabilities of atoms arising from not only mechanical but also electric loading, i.e., multi-physics instabilities. The criterion for such multi-physics instabilities in ferroelectrics has been proposed by extending the original mechanical instability analysis (Shimada et al. 2012). In addition to the original framework, here the total energy of the system Π consists of not only the potential energy Φ and the work done by external load W, but also the electro-static energy due to external electric field V_{elec},

$$\Pi = \Phi + W + V_{elec} \tag{17.18}$$

By following the same manner as the original theory, the Hessian matrix to be solved **H** is now re-formulated as

$$H_{mn} = \left.\frac{\partial^2 \Phi}{\partial R_m \partial R_n}\right|_{R=R_0} + \left.\frac{\partial^2 V_{elec}}{\partial R_m \partial R_n}\right|_{R=R_0} \tag{17.19}$$

Therefore, the eigenvalue of the re-formulated Hessian matrix can be a criterion for ferroelectric systems that essentially include a strong interaction with both mechanical and electric loading.

This criterion was applied to the switching of 180° domain walls (DWs) in ferroelectric PbTiO$_3$ under external electric field (Shimada et al. 2012), as shown in Fig. 17.8a. This simulation model with periodic boundary conditions contains a 180° DW at the center of cell. The left side of DW shows spontaneous polarization in the +z direction while that of the right side is the opposite −z direction. When the external electric field is applied in the +z direction, spontaneous polarization (referred as ferro-electric distortion δ_{FE} here) of the right side of DW (denoted as plane 1–4) smoothly increases, as shown in Fig. 17.8b. When the electric field reaches the critical value of $E_c = 4.225$ MV/cm, δ_{FE} changes from the negative to positive value, indicating that spontaneous polarization switches from −z to +z, i.e., the domain switching occurs. The minimum eigenvalue, as a criterion based on the above extended the-
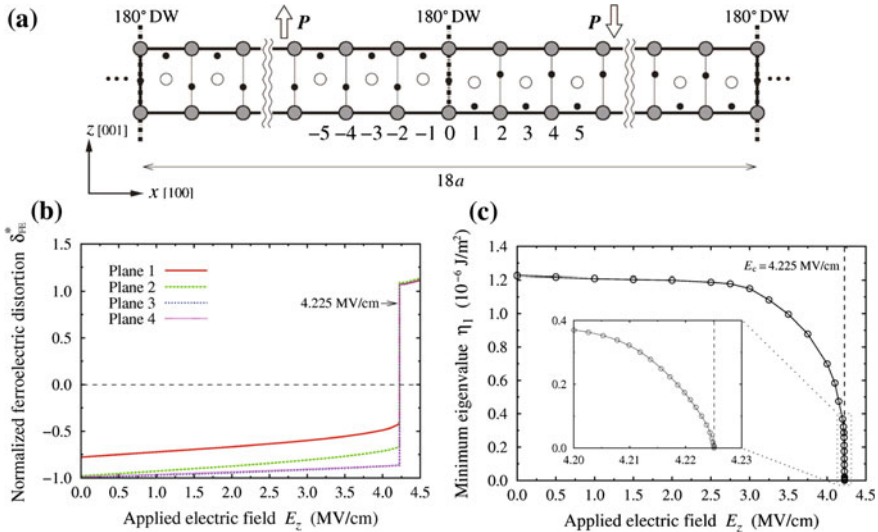
Fig. 17.8 Computational results for domain switching in ferroelectric PbTiO$_3$. **a** Simulation supercell for 180° domain walls in ferroelectric PbTiO$_3$. **b** Ferroelectric distortion (spontaneous polarization) as a function of external electric field. **c** Minimum eigenvalue as a function of applied electric field (Shimada et al. 2012)

ory, smoothly decreases with increasing electric field, as shown in Fig. 17.8c. The minimum eigenvalue reaches zero (criterion) at the field of 4.225 MV/cm, which corresponds to the point where domain switching starts. This consistency therefore demonstrates that the criterion based on the extended theory can successfully capture (ferro-)electric instabilities in such ionic systems.

The instability criterion has also been extended to magnetic (spin-lattice) systems (Shimada et al. 2015). The potential energy of the system with magnetic moments, such as ferromagnetic Fe, is described by not only the atomic coordinates, $\boldsymbol{R}$, but also magnetic moments, $\boldsymbol{m}$, and is given by

$$\Phi = \Phi(\boldsymbol{R}, \boldsymbol{m}), \tag{17.20}$$

where

$$\boldsymbol{m} \equiv^t (m_x^1, m_y^1, m_z^1, m_x^2, m_y^2, m_z^2, \ldots, m_x^N, m_y^N, m_z^N) \tag{17.21}$$

Here, m_i^α denotes the magnetic moment of atom α in the i direction. Since the DOFs of magnetic moment in the system is $3N$, the total number of DOFs including atomic and spin DOFs is now $M = 6N - 6$. Here, an arbitrary deformation and/or perturbation of the magnetic moment of the system can be represented by a change in the following M-dimensional vector $\boldsymbol{X}$ consisting of all DOFs,

$$\begin{aligned} \boldsymbol{X} \equiv^t \ &(r_z^2, r_y^3, r_z^3, r_x^4, r_y^4, r_z^4, \ldots, r_x^N, r_y^N, r_z^N) \\ &m_x^1, m_y^1, m_z^1, m_x^2, m_y^2, m_z^2, \ldots, m_x^N, m_y^N, m_z^N) \end{aligned} \tag{17.22}$$

The total energy of the spin-lattice system Π now consists of not only the potential energy Φ and the work done by external load W, but also the magnetostatic energy due to external magnetic field V_{mag},

$$\Pi = \Phi + W + V_{\text{mag}} \tag{17.23}$$

By following the same manner as the original concept, the Hessian matrix to be solved $\boldsymbol{H}$ is now re-written as

$$H_{mn} = \left. \frac{\partial^2 \Phi}{\partial X_m \partial X_n} \right|_{\boldsymbol{X} = \boldsymbol{X}_0} + \left. \frac{\partial^2 V_{\text{mag}}}{\partial X_m \partial X_n} \right|_{\boldsymbol{X} = \boldsymbol{X}_0} \tag{17.24}$$

Again, the eigenvalue of the re-formulated Hessian matrix can be a criterion for a magnetic system. This extended criterion was applied to magnetization switching in ferromagnetic Fe under external magnetic field, as shown in Fig. 17.9. The magnetic moment in Fe is initially along $+z$ direction ($\theta = 0$ rad; point A in Fig. 17.9a). When the external magnetic field is applied in $+x$ direction, the magnetic moment slightly rotates (point B). When the magnetic field reaches at the coercive field H_c, the magnetic moment suddenly rotates from $+z$ to $+x$ direction (points C-D; see

Fig. 17.9 Computational results for magnetization switching in ferromagnetic iron. **a** Magnetic moment as a function of external magnetic field. **b** Magnetic configurations under applied magnetic fields. **c** Minimum eigenvalue of criterion as a function of magnetic field. **d** Unstable mode of magnetic moments under the coercive field (Shimada et al. 2015)
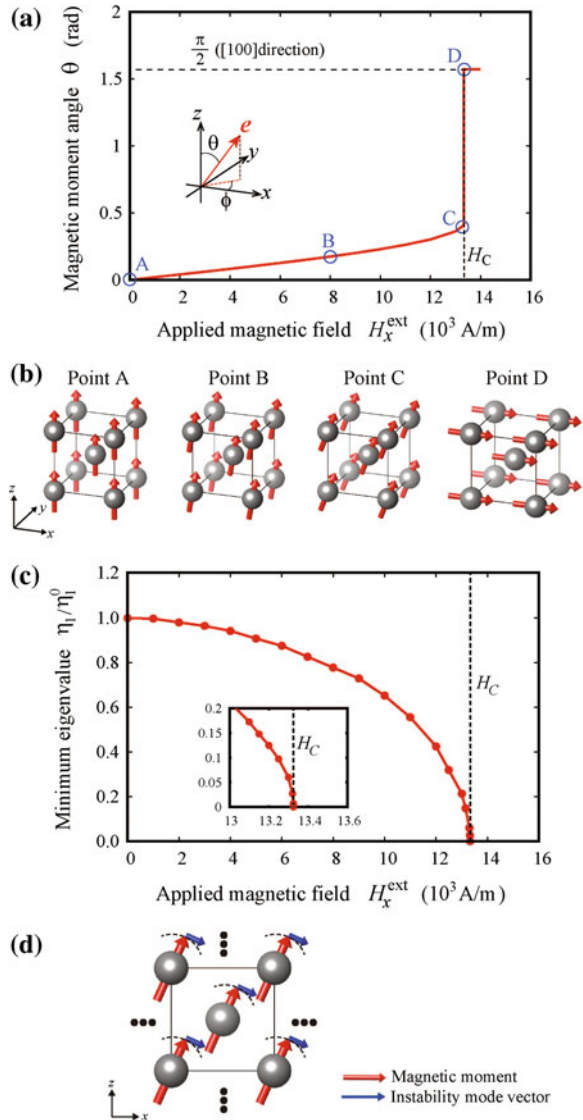
also Fig. 17.9b), i.e., magnetization switching occurs. The minimum eigenvalue, as a magnetic criterion based on the extended theory, smoothly decreases with increasing magnetic field (see Fig. 17.9c). The minimum eigenvalue finally becomes zero (criterion) at the coercive field of H_c, which corresponds to the points C–D where magnetization switching occurs. This agreement shows that the criterion based on the extended theory can successfully describe the magnetic instabilities in spin-lattice

systems. In addition, the unstable mode of magnetic moments shown in Fig. 17.9d demonstrates the rotation of spins toward the $+x$ direction, which correctly represents the behavior of magnetization switching shown in Fig. 17.9b.

17.5 Conclusions

This review covered the state-of-the-art theory of "fracture mechanics of atomic structures" that provides a rigorous description of mechanical instabilities in arbitrary atomic structures under any external loading/constraint. The theory gives the critical instability condition by positivity of the minimum eigenvalue of the Hessian matrix of the total energy with respect to degrees of freedom of the system as well as the fracture mode at the onset of instability. The theory successfully provides atomistic insights into fracture in various atomic/nanoscale structures including nanocracks, interface edges, defects, amorphous and non-crystalline structures. The review concludes with recent advances of the theory extended to complicated and multi-functional systems including large-scale, finite temperature, and multi-physics instabilities in (ferro-)electric and magnetic materials as functional fracture. Such extension of the instability theory for multi-physics phenomena can open up a new discipline underlying between material strength and physical properties.

References

Bažant ZP (2002) Concrete fracture models: testing and practice. Eng Frac Mech 69:165–205
Born M, Huang K (1954) Dynamical theory of crystal lattices. Oxford University Press, Oxford
Buehler MJ, Gao H (2006) Dynamical fracture instabilities due to local hyperelasticity at crack tips. Nature 439:307–310
Černý M, Šob M, Pokluda J, Šandra P (2004) Ab initio calculation of ideal tensile strength and mechanical stability in copper. J Phys Condens Matter 16:1045–1052
Dmitriev SV, Kitamura T, Li J, Umeno Y, Yashiro K, Yoshikawa N (2005a) Near-surface lattice instability in 2D fiber and half-space. Acta Mater Sci 53:1215–1224
Dmitriev SV, Li J, Yoshikawa N, Shibutani Y (2005b) Theoretical strength of 2D hexagonal crystals: application to bubble raft indentation. Philos Mag 85:2177–2195
Dombard AJ (2007) Planetary science crack under stress. Nature 447:276–277
Hill R, Milstein F (1997) Principles of stability analysis of ideal crystals. Phys Rev B 15:3087–3096
Holland D, Marder M (1999) Crack and atoms. Adv Mater 11:793–806
Kermode JR, Albaret T, Sherman D, Bernstein N, Gumbsch P, Payne MC, Csányi G, de Vita A (2008) Low-speed fracture instabilities in a brittle crystal. Nature 455:1224–1227
Kitamura T, Yashiro K, Ohtani R (1997) Atomic simulation on deformation and fracture of nano-single crystal of nickel in tension. JSME Int J Ser A 40:430–435

Kitamura T, Umeno Y, Fushino R (2004a) Instability criterion of inhomogeneous atomic system. Mater Sci Eng A 379:229–233

Kitamura T, Umeno Y, Tsuji N (2004b) Analytical evaluation of unstable deformation criterion of atomic structure and its application to nanostructure. Comp Mater Sci 29:499–510

Kitamura T, Yashiro K, Ohtani R (1998) Mesoscopic dynamics of fracture. Computational materials design. Springer, Berlin, pp 120–130

Kubo A, Albina JM, Umeno Y (2013) Atomistic study of stress-induced switch-ing of 90° ferroelectric domain walls in PbTiO3: size, temperature and structural effect. Model Simul Mater Sci Eng 21(065):019

Li J, van Vliet KJ, Zhu T, Yip S, Suresh S (2002) Atomistic mechanisms governing elastic limit and incipient plasticity in crystals. Nature 418:307–310

Li J, Ngan AHW, Gumbsch P (2003) Atomic modeling of mechanical behavior. Acta Mater 51:5711–5742

Liebowitz H (1968) Fracture—an advanced treatise. Academic Press, New York

Livne A, Bouchbinder E, Svetlizky I, Fineberg J (2010) The near-tip fields of fast cracks. Science 327:1359–1363

Luo W, Roundy D, Cohen ML, Morris JW (2002) Ideal strength of bcc molybdenum and niobium. Phys Rev B 66(094):110

Milstein F (1971) Theoretical strength of a perfect crystal. Phys Rev B 3:1130–1141

Milstein F (1980) Theoretical elastic behaviour of crystals at large strains. J Mater Sci 15:1071–1084

Nalla RK, Kinney JH, Richie RO (2003) Mechanistic fracture criteria for the failure of human cortical bone. Nat Mater 2:164–168

Pons AJ, Karma A (2010) Helical crack front instability in mixed-mode fracture. Nature 464:85–89

Rubin AM (1995) Propagation of magma-field cracks. Annu Rev Earth Planet Sci 23:287–336

Shimada T, Okawa S, Minami S, Kitamura T (2008) Development of efficient instability analysis method for atomic structures using linear elements and its application to amorphous metal (in Japanese). Trans Jpn Soc Mech Eng A 74:1328–1335

Shimada T, Okawa S, Minami S, Kitamura T (2009a) Development of efficient instability analysis method for atomic structures using linear elements and its application to amorphous metal. J Solid Mech Mater Eng 3(5):807–818

Shimada T, Okawa S, Minami S, Kitamura T (2009b) Simplified evaluation of mechanical instability in large-scale atomic structures. Mater Sci Eng A 513–514:166–171

Shimada T, Kondo T, Sumigawa T, Kitamura T (2010a) Mechanical instability criterion of dislocation structures based on discrete dislocation dynamics. Trans Jpn Soc Mech Eng A 76:1721–1728

Shimada T, Okawa S, Kitamura T (2010b) Simplified analysis of mechanical in-stability three-dimensional atomic components and its application to nanoscale crack. J Solid Mech Mater Eng 4(7):1071–1082

Shimada T, Sakamoto H, Kitamura T (2012) Development of multi-physics in-stability criterion for atomic structures and application to domain switching in ferroelectrics under external electric field. J Soc Mater Sci 61:155–161

Shimada T, Kitamura T (2014) Multi-physics properties in ferroelectric nanostructure. Bull JSME 1(2):SMM0009-SMM0009

Shimada T, Ouchi K, Ikeda I, Ishii Y, Kitamura T (2015) Magnetic instability criterion for spin-lattice systems. Comp Mater Sci 97:216–221

Song J, Curtin WA (2013) Atomic mechanism and prediction of hydrogen embrittlement in iron. Nat Mater 12:145–151

Umeno Y, Kitamura T, Tagawa M (2007) Mechanical instability in non-uniform atomic structure: application to amorphous metal. Mater Sci Eng A 462:450–455

Umeno Y, Shimada T, Kitamura T (2009) Instability mode analysis of dislocation nucleation from notch based on atomistic model (instability activation mechanism under finite temperature). Trans Jpn Soc Mech Eng A 75:1247–1254

Umeno Y, Shimada T, Kitamura T (2010) Dislocation nucleation in a thin Cu film from molecular dynamics simulations: instability activation by thermal fluctuations. Phys Rev B 82(104):108

van Vliet KJ, Li J, Zhu T, Yip S, Suresh S (2003) Quantifying the early stages of plasticity through nanoscale experiments and simulations. Phys Rev B 67(104):105

Wang J, Yip S, Phillpot SR, Wolf D (1993) Crystal instabilities at finite strain. Phys Rev Lett 71:4182–4185

Wang J, Li J, Yip S, Wolf D, Phillpot SR (1997) Unifying two criteria of born: elastic instability and melting of homogeneous crystals. Physica A 240:396–403

Wang J, Li J, Yip S, Phillpot SR, Wolf D (1995) Mechanical instabilities of homogeneous crystals. Phys Rev B 52:12,627–12,635

Warner DH, Curtin WA, Qu S (2007) Rate dependence of crack-tip processes predicts twinning trend in f.c.c. metals. Nat Mater 6:876–881

Yan Y, Kondo T, Shimada T, Sumigawa T, Kitamura T (2012) Criterion of mechanical instabilities for dislocation structures. Mater Sci Eng A 534:681–687

Yashiro K, Tomita Y (2010) Local lattice instability at a dislocation nucleation and motion. J Phys IV 11:Pr5-3-Pr5-10

Zhang P, Ma L, Fan F, Zeng Z, Peng C, Loya PE, Liu Z, Gong Y, Zhang J, Zhang X, Ajayan PM, Zhu T, Lou J (2014) Fracture toughness of graphene. Nat Commun 5:3782